16

Neutrino Masses and Oscillations

The Old Enigma.

The most enigmatic of elementary particles, neutrinos were postulated in 1930, but were not observed until a quarter of a century later. It took another forty years to determine that they are not massless.

Neutrinos are a ubiquitous if imperceptible part of our environment. Neutrinos created in the Big Bang together with the cosmic background radiation pervade the entire Universe. The Sun is a poweful source of MeV neutrinos. Neutrinos in the GeV range are created when cosmic rays strike the atmosphere, 15 kilometers or so above the Earth's surface. Every nuclear reactor emits antineutrinos copiously. High-energy neutrinos are regularly produced at accelerators through particle decay and carefully fashioned magnetic fields can focus produced unstable charged particles to create neutrino beams.

Traditionally, efforts were made to set upper limits on the masses of the neutrinos associated with the electron, muon, and tau lepton. As explained in Chapter 6, if the electron neutrino were sufficiently massive the electron spectrum in tritium beta decay would be distorted near the end point. This prompted many painstaking measurements over the past thirty years. The expression for the spectrum actually depends on the square of the neutrino mass and the best fits can return unphysical, negative values for this. Current results give $-1.1 \pm 2.4\ \mathrm{eV}^2$.

The direct limits on the masses of the other neutrinos are not nearly so strong. The best direct limit on the mass of ν_μ is obtained from $\pi^+ \to \mu^+\nu_\mu$, which gives a 90% CL upper limit of 190 keV. The mass of ν_τ can be sought by studying τ decays of the sort $\tau^- \to 2\pi^-\pi^+\nu_\tau$ and $\tau^- \to 3\pi^-2\pi^+\nu_\tau$. If ν_τ is massive, the invariant mass spectrum of the charged pions will terminate below the mass of the τ. The best limit obtained to date is $m_{\nu_\tau} < 18.2$ MeV. These direct limits have been superseded. Massive neutrinos would affect the density fluctuations in the early Universe. Detailed measurements of the cosmic microwave background and other cosmological parameters indicate that the sum of the three neutrino masses must be less than about 0.6 eV.

16.1 The Nature of Neutrino Masses

Neutrinos may acquire their masses very differently from the way quarks and charged leptons do. The electron–positron system has four degrees of freedom, which we can represent by e_L, e_R, e_L^c, and e_R^c, where we have chosen to write e^c for e^+. For the neutrino we can write similarly ν_L, ν_R, ν_L^c and ν_R^c. To make a massive spin-one-half particle, we need both "left-handed" and "right-handed" pieces. For neutrinos we can suppose that the massive particle is a combination of the left-handed neutrino and the right-handed antineutrino:

$$N_1 = \nu_L + \nu_R^c. \tag{16.1}$$

This provides all the degrees of freedom required. A massive neutrino with only two degrees of freedom instead of four is called a Majorana neutrino.

The mass of the electron is described in the Lagrangian by the expression $m_e \bar{e} e = m_e(\bar{e}_L e_R + \bar{e}_R e_L)$. The mass term changes a left-handed electron into a right-handed electron, with amplitude m_e. Of course this is a colloquialism since the freely propagating electron cannot spontaneously change its angular momentum! The imprecision arises because $e_L = \frac{1}{2}(1 - \gamma_5)e$ describes a left-handed electron only in the ultrarelativistic limit. An electron emitted in beta decay has polarization, on average, $-v/c$.

While N_1 has the degrees of freedom required for a massive fermion, by combining a lepton with an antilepton we have broken lepton number conservation. If we tried the same thing with an electron, joining the left-handed electron with the right-handed positron, we would have broken charge conservation, something that is certainly impermissible. Whether lepton number is truly conserved is an experimental question.

There are a number of nuclides that are stable against both β^- and β^+ decay, but that are unstable against double beta decay. An example is Ge_{32}^{76}. Energy conservation forbids $\mathrm{Ge}_{32}^{76} \to \mathrm{Ga}_{31}^{76}\, e^+ \nu_e$ and $\mathrm{Ge}_{32}^{76} \to \mathrm{As}_{33}^{76}\, e^- \overline{\nu}_e$, but $\mathrm{Ge}_{32}^{76} \to \mathrm{Se}_{34}^{76}\, e^- \nu_e e^- \nu_e$ occurs with a half-life of about 1.5×10^{21} y. The neutrinoless double beta decay $\mathrm{Ge}_{32}^{76} \to \mathrm{Se}_{34}^{76} e^- e^-$ would violate lepton number. If ν_e is a Majorana particle, such a process is allowed.

Imagine this decay occurs through the intermediate virtual process $\mathrm{Ge}_{32}^{76} \to \mathrm{Se}_{34}^{76}\, W^- W^-$. One W decays to $e^- \overline{\nu}_{eR}$, where the antineutrino is virtual. If the neutrino is a Majorana particle, the $\overline{\nu}_{eR}$ can become ν_{eL}, indeed the two are components of a single massive particle. The ν_{eL} combines with the W^- to make the second e^-. The amplitude for this process is proportional to m_{ν_e}, so that observing it would establish a non-zero neutrino mass, and would show as well that lepton number is violated. The experimental lower limit on the half-life of Ge_{32}^{76} against neutrinoless double beta decay is about $1\text{–}2 \times 10^{25}$ y, though there is a controversial claim of observation at the lower end of this range.

The Standard Model together with Majorana neutrinos can accommodate quite naturally very small, but finite, neutrino masses. For an electron, the mass term changes a left-handed state into a right-handed state, with amplitude m_e, changing the weak isospin from $I_z = -1/2$ to $I_z = 0$. This is permissible because the electron interacts with the ubiquitous Higgs field, which has $I_z = \pm 1/2$ and which is non-zero everywhere.

Our Majorana neutrino N_1 behaves differently. To change ν_L ($I_z = 1/2$) to ν_R^c ($I_z = -1/2$) requires $\Delta I_z = 1$, more than the Higgs field supplies. Thus we expect this amplitude

to be zero or very, very small. Suppose, however, that in addition there is a right-handed neutrino, together with its conjugate, a left-handed antineutrino. Neither of these feels the weak force since they have weak-isospin zero. Together they can form a second Majorana neutrino,

$$N_2 = \nu_R + \nu_L^c. \tag{16.2}$$

To change from the left-handed piece of N_2 to the right-handed piece doesn't change I_z at all, since both pieces are neutral under weak isospin. There is no reason for this not to have a large amplitude since it does not break weak isospin symmetry and thus need not depend on the "low" mass scale at which electroweak symmetry is broken. The corresponding mass $M_{\rm big}$ might even be as large as 10^{15} GeV, the scale at which the strong and electroweak forces may be unified.

It is also possible for N_1 and N_2 to mix. In particular, the ν_L in N_1 can become ν_R in N_2 with a change $I_z = 1/2$, just as e_L becomes e_R. Indeed, we might anticipate an amplitude of the same scale, m. The same is true for the transition of N_2 to N_1. These results can be summarized in a mass matrix in which the first row and column refer to N_1 and the second to N_2:

$$\begin{pmatrix} 0 & m \\ m & M_{\rm big} \end{pmatrix} \tag{16.3}$$

where the 0 and $M_{\rm big}$ follow from the rule that $\Delta I_z = 1$ is disallowed, but $\Delta I = 0$ is unsuppressed. For $m << M_{\rm big}$, the eigenvalues of the matrix are nearly $M_{\rm big}$ and $-m^2/M_{\rm big}$. The negative sign has no physical significance; it corresponds to a mass $m^2/M_{\rm big}$. If we guess that $m = m_e$ and $M_{\rm big} = 10^{15}$ GeV, a value motivated by theories in which the strong and electroweak interactions are unified at a high mass scale, we get a neutrino mass of less than 10^{-12} eV, very small indeed. The lighter eigenstate is mostly the weakly interacting Majorana neutrino, while the heavier one is mostly the non-interacting Majorana neutrino:

$$\begin{aligned} |N_L\rangle &\approx |N_1\rangle - \frac{m}{M_{\rm big}}|N_2\rangle, \\ |N_H\rangle &\approx |N_2\rangle + \frac{m}{M_{\rm big}}|N_1\rangle. \end{aligned} \tag{16.4}$$

This means of generating two Majorana neutrinos, one with a very large mass and one with a very small mass, is known as the seesaw mechanism.

16.2 Neutrino Mixing

If neutrinos have mass, the leptonic system is quite analogous to the quark system. We thus expect that the weak eigenstates may not correspond to the mass eigenstates: there is a leptonic version of the Kobayashi–Maskawa matrix – the Maki–Nakagawa–Sakata matrix – connecting the two. For simplicity, consider just two species of neutrinos, ν_e, the

weak partner of the electron, and ν_μ, the weak partner of the muon. The mass eigenstates must be combinations of these two (later we consider the three-generation case):

$$\begin{aligned} |\nu_1\rangle &= \cos\theta_0|\nu_e\rangle - \sin\theta_0|\nu_\mu\rangle, \\ |\nu_2\rangle &= \sin\theta_0|\nu_e\rangle + \cos\theta_0|\nu_\mu\rangle, \end{aligned} \tag{16.5}$$

where ν_1 is the lighter state. We can always choose $0 \leq \theta_0 < \pi/2$ by redefining the states $|\nu\rangle \to -|\nu\rangle$, if necessary. When a beta decay produces a ν_e, its time development will be described by

$$|\nu_e(t)\rangle = e^{-iE_1t}\cos\theta_0|\nu_1\rangle + e^{-iE_2t}\sin\theta_0|\nu_2\rangle. \tag{16.6}$$

If the state has well-defined momentum $p \approx E >> M_1, M_2$, then its components have different energies

$$E_1 \approx p + \frac{M_1^2}{2p}; \qquad E_2 \approx p + \frac{M_2^2}{2p}. \tag{16.7}$$

After traveling a distance $L \approx t$, the two pieces will have a relative phase $(M_2^2 - M_1^2)L/(2E) = \Delta M^2 L/(2E)$. The probability that the ν_e will have become a ν_μ is easily determined to be

$$P_{\nu_e\to\nu_\mu}(t) = |\langle\nu_\mu|\nu_e(t)\rangle|^2 = \sin^2 2\theta_0 \sin^2\left(\frac{\Delta M^2 L}{4E}\right). \tag{16.8}$$

In practical units, the last factor is

$$\sin^2\left(1.27\frac{\Delta M^2(\text{eV}^2)L(\text{km})}{E(\text{GeV})}\right). \tag{16.9}$$

These oscillations are similar to those in the K^0–$\overline{K}^0$ and B^0–$\overline{B}^0$ systems. There the oscillation is manifested in the variation in the sign of charged leptons emitted in semileptonic decays. Here it is the type of lepton itself that varies. The specific phenomenon observed depends on the energy of the neutrino that is oscillating. Antineutrinos generated by beta decays in nuclear reactors have energies in the MeV range. If these antineutrinos oscillate from electron-type to muon- or tau-type, their energies will be too low to produce in a detector the associated charged leptons. What would be measurable would be simply a drop in the number of charged-current reactions. The neutrinos would seem to disappear.

A neutrino beam generated by decaying pions will be dominantly ν_μ or $\overline{\nu}_\mu$ depending on the sign of the pions. Its charged-current interactions will regenerate muons. If, however, the beam oscillates to electron- or tau-type neutrinos, the corresponding charged leptons could be produced. Such an experiment would establish oscillations by appearance.

16.3 Solar Neutrinos

The earliest indications of neutrino oscillations came in solar neutrino experiments. The initial step in the fusion cycle that powers the Sun is the weak process $pp \rightarrow de^{+}\nu_e$. Because the total rate of energy production is proportional to the rate at which this reaction occurs, there is little uncertainty about the neutrino flux at the Earth's surface from this source. This turns out to be about 6×10^{10} cm^{-2} s^{-1}. See Exercise 16.1. These neutrinos have energies below 0.5 MeV and are thus below threshold for charged-current interactions except with a few nuclides. The next most copious source of solar neutrinos is electron capture on Be^7: $Be^7 e^{-} \rightarrow Li^7 \nu_e$, with discrete neutrino energies near 0.4 MeV and 0.9 MeV. The Be^7 are generated in the process $He^4 + He^3 \rightarrow Be^7 + \gamma$. The third significant source of solar neutrinos is the decay $B^8 \rightarrow Be^{8*} e^{+} \nu_e$, which produces neutrino energies up to nearly 18 MeV. The B^8 are themselves produced via $Be^7 + p \rightarrow B^8 + \gamma$. The beta-decay product B^8 decays to two alpha particles, and is thus incorporated into the overall burning of hydrogen into helium. Even though the flux of the B^8 neutrinos is smaller by about 10^{-4} than those from the pp reaction, their high energy and correspondingly large cross sections makes them very important in solar neutrino experiments.

The solar neutrinos can be detected if they are captured by isotopes like Cl^{37} ($\nu_e Cl^{37} \rightarrow e^{-} Ar^{37}$) and Ga^{71} ($\nu_e Ga^{71} \rightarrow e^{-} Ge^{71}$), which then become radioactive with subsequent decays that can be observed. The threshold for the former capture is 814 keV, while for the latter it is 233 keV. As a result, chlorine experiments are blind to the pp reaction, while gallium experiments can detect it. The chlorine experiments are dominated by neutrinos from B^8 and Be^7. They were pioneered by Ray Davis at the Homestake Mine in South Dakota, starting back in the 1960s (**Ref. 16.1**).

In 1968 Davis's team reported an upper limit of 3 SNU (1 SNU – solar neutrino unit – is 10^{-36} neutrino captures per atom per second) for a chlorine experiment. The prediction of the rate from solar models is difficult and at the time the expected total rate was 20 SNU, 90% of which was due to B^8. To make this measurement, Davis needed to isolate about one atom of Ar^{37} produced each day in a vat of 3.9×10^5 liters of C_2Cl_4 located 1.5 km underground. As shown in Table 16.1, the contemporary prediction is 7.6 SNU and the 1998 result from the Homestake experiment is 2.56 SNU.

Gallium experiments were pursued by the GALLEX collaboration from 1991 to 1997 at the Gran Sasso National Laboratory in the Gran Sasso d'Italia in the Abruzzo region 150 km east of Rome and by the SAGE collaboration at Baksan, in Russia. The cumulative result from GALLEX was 77.5 SNU with a precision of about 10%. This was about 60% of the predicted rate of 128 SNU. The SAGE result was similar. The GALLEX experiment was succeeded by GNO, the Gallium Neutrino Observatory, where the rate was measured to be near 63 SNU.

An alternative to detecting individual transmuted atoms relies on Cherenkov light from charged-current reactions induced by the neutrinos. Because an enormous target is required to obtain sufficient rate, the natural medium is water. The leading experiments using this technique have been located at the Komioka Mozumi mine in Japan. The Kamioka Nucleon Decay Experiment (Kamiokande) was upgraded to a neutrino detector just in time to catch neutrinos from the supernova SN1987a. After its run from 1987 to 1995, it was succeeded

Table 16.1. *Predictions for the solar neutrino flux from J. N. Bahcall, M. H. Pinsonneault, and S. Basu, Astrophys. J.* **555***, 990 (2001) and corresponding experimental results, adapted from the summary of N. Nakamura in the 2006 Review of Particle Physics. The gallium experiments are in good agreement with one another. The chlorine and gallium experiments are sensitive only to the charged current. The Kamiokande and Super-Kamiokande experiments measure the elastic scattering* $\nu e^- \to \nu e^-$*, which has contributions from both charged and neutral currents. The solar neutrino unit (SNU) is* 10^{-36} *neutrino captures per atom per second.*

Solar Sources:	^{37}Cl (SNU)	^{71}Ga (SNU)	^{8}B ν flux (10^6 cm^{-2} s^{-1})
$pp \to de^+\nu_e$		69.7	
^{7}Be $e^- \to ^{7}$ Liν_e	1.15	34.2	
^{8}B $\to ^{8}$ Be* $e^+\nu_e$	5.67	12.1	5.05
Other	0.68	11.9	
Total	$7.6^{+1.3}_{-1.1}$	128^{+9}_{-7}	$5.05^{+1.01}_{-0.80}$
Experiment:			
Homestake	$2.56 \pm 0.16 \pm 0.16$		
GALLEX		$77.5 \pm 6.2^{+4.3}_{-4.7}$	
GNO		$62.9^{+5.5}_{-5.3} \pm 2.5$	
SAGE		$70.8^{+5.3\ +3.7}_{-5.2\ -3.2}$	
Kamiokande			$2.80 \pm 0.19 \pm 0.33$
Super-Kamiokande			$2.35\ \pm\ 0.02 \pm 0.08$

by the 50-kton detector Super-Kamiokande. The threshold for observability for both was several MeV and these experiments were thus dominated by neutrinos from B^8 decay. Both experiments found fluxes about half the expected level of 5×10^6 cm^{-2} s^{-1} and showed that the neutrinos indeed came from the direction of the Sun.

Every one of these techniques is extremely challenging because of the small rates and large detectors employed. What is striking is that the results of all these experiments tell about the same story: about one-third to one-half the expected rate of neutrino interactions is actually observed. See Table 16.1.

The solar abundances of elements like beryllium and boron must be deduced from solar models and this added some doubt to the predictions for these contributions to the solar neutrino flux. However, there was good agreement between the various calculations that had been done to estimate these abundances. This made it hard to dismiss the results from the Cherenkov and chlorine experiments. Moreover, fully half of the reaction rate expected in the gallium experiments is due to the *pp* reaction, about whose rate there could be little doubt since it is directly connected to the total luminosity of the Sun.

The discrepancy between the expected and observed rates for solar neutrino experiments was consistent and persistent. Attempts to blame the problem on solar models were weakened by the GALLEX, GNO, and SAGE results. What remained suggested strongly that there are neutrino oscillations involving electron neutrinos.

For mixing to play a role, it would seem that $\Delta m^2 L/E$ (where $L = 1.5 \times 10^{11}$ m is the distance from the Earth to the Sun) would have to be not too small, i.e. $\Delta m^2 > 10^{-12}$ eV^2 so the oscillation length would not be large compared to L. In the limit that there were many oscillations between the Sun and the Earth, we would expect that averaging over an energy spectrum would replace the oscillation in L by its average, 1/2:

$$P_{\nu_e \to \nu_\mu} = \frac{1}{2} \sin^2 2\theta_0, \tag{16.10}$$

so that at most half the neutrinos could disappear. With three species, the limit would be two-thirds disappearing. In fact, the behavior of solar neutrinos is more complex because they must first pass from the Sun's core to its edge before entering the void.

16.4 MSW Effect

If there is mixing between ν_e and, say, ν_μ, the combinations that are eigenstates in free space will not remain eigenstates when passing through matter. This is completely analogous to the phenomenon of regeneration in the neutral K system. There regeneration occurs because K^0 and $\overline{K}^0$ have different forward scattering amplitudes on nuclei. In the neutrino system the corresponding difference is between the forward elastic scattering of ν_e on electrons and ν_μ on electrons. This regeneration is known as the Mikheyev–Smirnov–Wolfenstein (MSW) effect. While $\nu_\mu e$ elastic scattering occurs only through the neutral current, $\nu_e e$ elastic scattering has a contribution from the charged-current process in which the incident electron-neutrino is transformed into an electron and the struck electron becomes itself an electron-neutrino. This interaction is described by the ordinary V-A theory

$$\frac{G_F}{\sqrt{2}} \overline{\nu}_e \gamma_\mu (1 - \gamma_5) e \, \overline{e} \gamma^\mu (1 - \gamma_5) \nu_e = \frac{G_F}{\sqrt{2}} \overline{\nu}_e \gamma_\mu (1 - \gamma_5) \nu_e \, \overline{e} \gamma^\mu (1 - \gamma_5) e \tag{16.11}$$

where the re-ordering follows from an algebraic identity for the gamma matrices known as a Fierz transformation. For electrons at rest, the last factor is important only for $\mu = 0$, when it gives the electron density, N_e. Acting on a left-handed neutrino, $1 - \gamma_5$ is simply 2 and the interaction is seen to be equivalent to a potential energy for neutrinos $V = \sqrt{2} G_F N_e$.

In the end, a complete analysis of neutrino mixing requires considering three neutrino species, but for the MSW effect a two-state approximation is adequate. What we call here ν_μ is, in fact, a linear combination of ν_μ and ν_τ.

For neutrinos, where the mass is apparent in the relation $E \approx p + \frac{1}{2}M^2/p$, the mass-squared matrix is of interest. The effect of the extra scattering of ν_e is to add to its diagonal element in this matrix the quantity $A = (E+V)^2 - E^2 \approx 2EV$

$$A = 2\sqrt{2}G_F N_e E = 0.76 \times 10^{-7}\text{eV}^2 \times \rho \left[\text{g cm}^{-3}\right] \times E\,[\text{MeV}] \times 2Y_e, \qquad (16.12)$$

where ρ is the mass density and the number of electrons per nucleon is Y_e. No other element of the mass-squared matrix is affected. The ν_e component of a mixed neutrino picks up an extra phase $\frac{1}{2}AL/E = \sqrt{2}G_F N_e L = 0.383 \times 10^{-3}\rho\left[\text{g cm}^{-3}\right] Y_e L\,[\text{km}]$ in traversing a distance L. If the material is hydrogen with a density of 1 g cm^{-3}, a full cycle is accumulated in a distance of 1.6×10^4 km, a bit more than the diameter of the Earth.

The mixing that results in the eigenstates $|\nu_1\rangle$ and $|\nu_2\rangle$ with masses squared M_1^2 and M_2^2 without the matter effect is described by

$$\mathbf{M^2} = \frac{M_2^2 - M_1^2}{2}\begin{pmatrix} -\cos 2\theta_0 & \sin 2\theta_0 \\ \sin 2\theta_0 & \cos 2\theta_0 \end{pmatrix}, \qquad (16.13)$$

where we drop the common diagonal term equal to the average mass squared. Multiplication verifies that the mixtures $|\nu_1\rangle$ and $|\nu_2\rangle$ are indeed eigenvectors of this matrix. Because the energy of a neutrino with momentum p is very nearly $p + \frac{1}{2}M^2/p$ we can write a Schrödinger equation for the state $|\psi\rangle = C_e|\nu_e\rangle + C_\mu|\nu_\mu\rangle$ as

$$i\frac{d}{dt}\begin{pmatrix} C_e \\ C_\mu \end{pmatrix} = \frac{1}{2E}\mathbf{M}^2\begin{pmatrix} C_e \\ C_\mu \end{pmatrix}. \qquad (16.14)$$

This system is analogous to a spin-one-half particle (whose spin is $\boldsymbol{\sigma}$) in a magnetic field with $\mathbf{B} \propto \cos 2\theta_0 \hat{\mathbf{z}} - \sin 2\theta_0 \hat{\mathbf{x}}$ since $\boldsymbol{\sigma}\cdot\mathbf{B}$ has the same form as $\mathbf{M}^2$. The electron-neutrino is analogous to the state whose spin is aligned with the magnetic field and the muon-neutrino is analogous to the state anti-aligned with it. The eigenstate $|\nu_1\rangle$ is the up state rotated by $2\theta_0$ about the y axis. Semiclassically, the spin precesses around the direction of the magnetic field. See Figure 16.1.

The extra elastic scattering of ν_e on electrons with density N_e changes the mass-squared matrix, again with the average diagonal term removed, to

$$\mathbf{M}^2{}_{eff} = \frac{\Delta M_0^2}{2}\begin{pmatrix} -\cos 2\theta_0 + \frac{A}{\Delta M_0^2} & \sin 2\theta_0 \\ \sin 2\theta_0 & \cos 2\theta_0 - \frac{A}{\Delta M_0^2} \end{pmatrix}, \qquad (16.15)$$

where $\Delta M_0^2 = M_2^2 - M_1^2$ is the splitting of the squares of the masses in vacuum. We can rewrite this in a form analogous to that for vacuum

$$\mathbf{M}^2{}_{eff} = \frac{\Delta M_{N_e}^2}{2}\begin{pmatrix} -\cos 2\theta_{N_e} & \sin 2\theta_{N_e} \\ \sin 2\theta_{N_e} & \cos 2\theta_{N_e} \end{pmatrix}, \qquad (16.16)$$

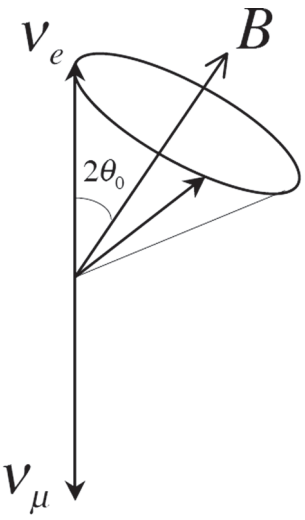

Figure 16.1. The analog between neutrino oscillations and precession of a spin-one-half particle in a magnetic field. A neutrino created as a ν_e (analogous to spin up) precesses about an axis at an angle $2\theta_0$. The precession gives oscillating fractions of ν_e and ν_μ, supposing these to be the mixed species. A fraction $\cos 2\theta_0$ of the spin is projected along the "field" direction. On average, the components perpendicular to the field vanish. If we project the average component back along the electron-neutrino's direction, we find a fraction $\cos^2 2\theta_0$. If we take this semiclassical expectation value to represent the probability $P_{\nu_e\to\nu_e} - P_{\nu_e\to\nu_\mu} = 1 - 2P_{\nu_e\to\nu_\mu}$ we find that $P_{\nu_e\to\nu_\mu} = \frac{1}{2}\sin^2 2\theta_2$. This agrees with the time-dependent expression, Eq. (16.8), when we average over a range of L that encompasses many cycles, corresponding to many cycles of the "spin" around the "magnetic field."

where now $\Delta M^2_{N_e}$ is the splitting of the squares of the eigenmasses in the medium. Identifying the two expressions for the mass matrix in matter we find the relations

$$\begin{aligned} \Delta M^2_{N_e} \sin 2\theta_{N_e} &= \Delta M^2_0 \sin 2\theta_0 \\ A &= \Delta M^2_0 \cos 2\theta_0 - \Delta M^2_{N_e} \cos 2\theta_{N_e}. \end{aligned} \tag{16.17}$$

This is shown geometrically in Figure 16.2.

If we imagine a hypothetical neutrino beginning at t_0 where the electron density is $N_e(t_0)$ in the lower-mass eigenstate $|\nu_1, N_e(t_0)\rangle$ (defined by the angle $\theta_{N_e(t_0)}$) and proceeding through matter whose density changes only gradually, we can expect the state to remain in the lower-mass eigenstate so that at time t it is $|\nu_1, N_e(t)\rangle$. This adiabatic evolution is analogous to the magnetic moment of the spin-1/2 particle following a gradual change in $\boldsymbol{B}$.

Physical neutrinos are produced not in mass eigenstates, but in "flavor" eigenstates because they arise from weak interactions. To follow the evolution of a neutrino that begins at the center of the Sun as $|\nu_e\rangle$ where the electron density is N_e, we project $|\nu_e\rangle$ along the "magnetic field" at the initial density, introducing a factor $\cos 2\theta_{N_e}$. See Figure 16.3. As the neutrino moves from the center of the Sun to the periphery, the density decreases and the orientation of the "magnetic field" gradually moves to the direction for vacuum

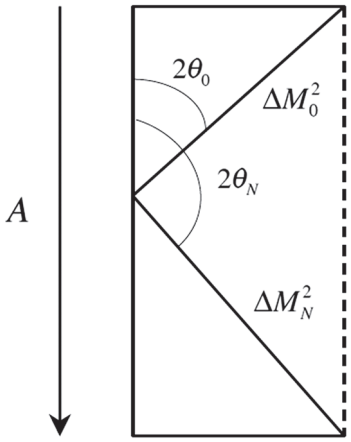

Figure 16.2. The relationship between the vacuum mixing angle, θ_0, and the mixing angle in matter, θ_N, and the mass splittings in vacuum and in matter. The quantity $A = 2\sqrt{2}G_F N_e E$, which is proportional to the electron density N_e and to the neutrino energy E, arises from the charged-current scattering in $\nu_e e \to \nu_e e$. As displayed in the figure, $\Delta M_0^2 \sin 2\theta_0 = \Delta M_N^2 \sin 2\theta_N$. If A is small, $\theta_0 \approx \theta_N$. If A is very large $2\theta_N \approx \pi$. When $\theta_N = \pi/2$, the mass splitting in matter is at its minimum. Note that in this figure, $\cos 2\theta_N < 0$.

mixing. In this adiabatic description, only the component along the magnetic field matters. The components transverse to it average to zero. When the neutrino finally exits the Sun, its "neutrino spin" direction is aligned with the magnetic field for vacuum mixing. On the passage from the Sun to the Earth this projection is unchanged: the actual vector just continues to precess about this average orientation. To determine its flavor content we finally project onto the ν_e direction. Altogether, the projections give $\cos 2\theta_{N_e} \cos 2\theta_0$. Equating this to $P_{\nu_e \to \nu_e} - P_{\nu_e \to \nu_\mu} = 1 - 2P_{\nu_e \to \nu_\mu}$ we find the adiabatic, and time averaged, prediction for the transformation from ν_e to ν_μ:

$$P_{\nu_e \to \nu_\mu} = \frac{1}{2}(1 - \cos 2\theta_{N_e} \cos 2\theta_0). \tag{16.18}$$

Of course in the limit of low matter density, $\theta_{N_e} \to \theta_0$ and this reduces to the vacuum expression. On the other hand, if the product of the energy and the initial density is large, then $\cos 2\theta_{N_e} \to -1$. The resulting transition probability is $P_{\nu_e \to \nu_\mu} = \frac{1}{2}(1 + \cos 2\theta_0) = \cos^2 \theta_0$, so that if the vacuum mixing angle were small, ν_e would be nearly certain to emerge as ν_μ.

As long as the spin precesses rapidly around the magnetic field, compared to the rate at which the direction of the magnetic field changes, this is a compelling argument. The precession frequency is proportional to $\Delta M_{N_e}^2$, which is smallest when $\sin 2\theta_{N_e} = 1$, i.e. when

$$\cos 2\theta_0 = \frac{A}{M_2^2 - M_1^2}. \tag{16.19}$$

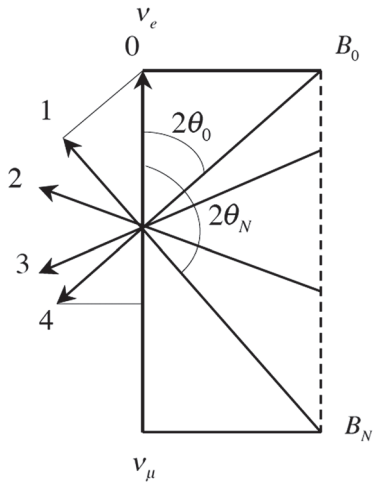

Figure 16.3. In the adiabatic approximation, the neutrino follows the magnetic field, which rotates as the electron density varies. The solar neutrino is produced as ν_e. If $\Delta M^2/2E$ is large enough, we can ignore the precession of the "spin" and look just at its projection along the "magnetic field." The neutrino produced at "0," is projected along the axis defined by the mixing angle for the density at the center of the Sun, B_N, at "1." As the density decreases, the direction of the "magnetic field" in the solar matter changes, as in "2" and "3," finally reverting to the vacuum direction, shown as "4." In the example shown here, the neutrino is then more aligned with the ν_μ direction than the original ν_e direction. It is clear, referring to a previous figure, that this will happen only if $A = 2\sqrt{2}G_F N_e E$ is sufficiently large. Following the geometry here, we find that $P_{\nu_e \to \nu_\mu} = \frac{1}{2}(1 - \cos 2\theta_N \cos 2\theta_0)$.

Passing through such a "resonance region" the spin may no longer follow the field and transitions from $|\nu_1(t)\rangle$ to $|\nu_2(t)\rangle$ become much more likely. Whether the adiabatic approximation applies depends on whether the direction of the "magnetic field," i.e. the matter density, changes gradually enough relative to the precession frequency, $\Delta M^2/2E$.

In the Sun, neutrinos are produced near the core, where the density is of order 130 $\mathrm{g\,cm^{-3}}$ and the atomic composition gives $Y_e = 0.67$. For a 1 MeV neutrino, A is about $1.3 \times 10^{-5}\ \mathrm{eV}^2$. Thus if $1.3 \times E(\mathrm{MeV}) \times 10^{-5}\ \mathrm{eV}^2$ is greater than $(M_2^2 - M_1^2)\cos 2\theta_0$, the construction shown in Figure 16.2 will make $2\theta_N > \pi/2$: Adiabatic evolution of a ν_e will end with the neutrino more likely to be "flipped" into ν_μ than to remain ν_e. For much lower energy neutrinos, A will be small and $\theta_N \approx \theta_0$. These neutrinos will not be "flipped." They emerge as electron-type neutrinos. See Exercise 16.4.

While the oscillation probability in vacuo depends only on $\sin 2\theta_0$ and thus is invariant under $\theta_0 \to \pi/2 - \theta_0$, the MWS effect depends on $\cos 2\theta_0$ and is not similarly invariant. Thus, in principle values of θ_0 between $\pi/4$ and $\pi/2$ must be considered as well as those from zero to $\pi/4$. This so-called "dark side" is disfavored by solar neutrino experiments because it gives $\cos 2\theta_0 < 0$ and according to Eq. (16.18) cannot suppress solar neutrinos by more than 50%.

16.5 MSW and the Solar Neutrino Problem

Once the MSW effect was included, three distinct solutions emerged for the solar neutrino problem defined by the results from chlorine and gallium experiments together with measurements by Kamiokande and Super-Kamiokande. Each solution corresponded to values for the mass splitting, $\Delta m^2_{\rm sol}$, and mixing angle $\theta_{\rm sol}$. One, termed the large mixing angle solution (LMA) had $\sin^2 2\theta_{\rm sol} \approx 0.5 - 1.0$ and $\Delta m^2_{\rm sol} \approx 10^{-5} - 3 \times 10^{-4}$ eV^2. A rather poorer fit, LOW (for low mass or perhaps low likelihood of being correct) was obtained with $\sin^2 2\theta_{\rm sol} \approx 1.0$ and $\Delta m^2_{\rm sol} \approx 10^{-7}$ eV^2. The small mixing angle solution had $\sin^2 2\theta_{\rm sol} \approx 10^{-2}$–$10^{-3}$ and $\Delta m^2_{\rm sol} \approx 5 \times 10^{-6}$ eV^2. In the LOW solution, the adiabatic approximation for MSW fails and a more complete calculation is required. In addition, solutions were possible with very low values of $\Delta m^2_{\rm sol}$, 10^{-12}–10^{-10} eV^2 and with large values of $\sin^2 2\theta_{\rm sol}$.

16.6 Cosmic-Ray Neutrinos

While the solar neutrino problem suggested that there were neutrino oscillations, convincing evidence came from an entirely different direction: cosmic rays. Indeed, there are two separate phenomena: solar neutrino mixing and atmospheric neutrino mixing, that is, mixing in neutrinos produced by collisions of cosmic rays in the atmosphere. It turns out that it is often possible to avoid considering three species of neutrinos and instead imagine that the solar neutrino and the atmospheric neutrino systems are two separate systems, each described by a two-neutrino pattern. The two phenomena occur at very different energy scales, MeV for solar neutrinos and GeV for atmospheric neutrinos.

In the hadronic showers of cosmic rays that strike the atmosphere, pions are created and decay to $\mu\nu$, and the muons subsequently decay to $e\nu\overline{\nu}$. In this way two ν_μs and one ν_e are generated for each charged pion created, ignoring the difference between neutrinos and antineutrinos.

The actual flux of particles created by the collisions high in the atmosphere is not so well known, so there is an advantage in comparing the ratio of neutrino events producing a muon in the detector to those producing an electron to the ratio expected from Monte Carlo simulations: $R = (\mu/e)_{DATA}/(\mu/e)_{MC}$. The absolute strength of the flux cancels in the ratio of the simulations. A number of experiments using water Cherenkov counters, including Kamiokande, the IMB (Irvine–Michigan–Brookhaven) experiment near Cleveland, Ohio, and Super-Kamiokande, observed values of R less than one, indicating that the ν_μ were somehow disappearing.

In 1998, the Super-Kamiokande team announced impressive evidence for neutrino oscillations **(Ref. 16.2)**. The ring of Cherenkov light produced by a muon in water has a sharper definition than that produced by the shower of an electron and the two categories can be reliably separated. More than 11,000 photomultiplier tubes viewed the central 22.5 kilotons of detector, in which events were required to begin. The Super-Kamiokande collaboration recorded more than 4000 events that were fully contained within the inner fiducial volume. The ratio R thus found differed substantially from unity, both for lower energy events

(visible energy below 1.33 GeV), with $R = 0.63 \pm 0.03 \pm 0.05$ and higher energy events, with $R = 0.65 \pm 0.05 \pm 0.08$.

From the Cherenkov light, it was possible to determine the direction of the incoming neutrino. Those that came from below must have been created in the atmosphere on the other side of the Earth, thousands of kilometers away. Those that came from above, were created relatively nearby. While the e-like events showed no particular directional dependence, the μ-like events that came from below were substantially depleted. The simplest interpretation is that the ν_μ oscillate to ν_τ with an oscillation wavelength comparable to the Earth's radius. Alternatively, the ν_μ might oscillate to some previously unknown neutrino type, a sterile neutrino that lacks interactions. Either way, for such a depletion to be observable, the mixing would have to be substantial. Since the ν_e seemed unaffected, it was sensible to fit the data assuming only ν_μ–ν_τ oscillations. The result was $\sin^2 2\theta_{\text{atm}} > 0.82$ and $5 \times 10^{-4}\ \text{eV}^2 < \Delta m^2_{\text{atm}} < 6 \times 10^{-3}\ \text{eV}^2$ at a 90% confidence level. With three times the exposure, Super-Kamiokande reported refined measurements: $\sin^2 2\theta_{\text{atm}} > 0.92$ and $1.5 \times 10^{-3}\ \text{eV}^2 < \Delta m^2_{\text{atm}} < 3.4 \times 10^{-3}\ \text{eV}^2$ at a 90% confidence level.

16.7 Reactor Neutrino Experiments

Reactor experiments produce antineutrinos, which accompany the beta particles emitted by fission products. Since the energies here are at most a few MeV, there is no possibility of observing the oscillation of $\overline{\nu}_e$ to $\overline{\nu}_\mu$ in a charged-current interaction: these neutrinos are below threshold for muon production. However, these oscillations would lead to a reduction in the number of charged-current events producing electrons. For sufficiently large mixing angles, such an effect would be observable by measuring the event rate with the reactor on and off, and comparing with the expected rate, based on the power produced by the reactor and an understanding of the decay chains associated with fission products. Such calculations are believed to be accurate at the few percent level. The domain of sensitivity in Δm^2 is set by equating $1.27\Delta m^2(\text{eV}^2)L(\text{m})/E(\text{MeV})$ to the observed limit on the oscillation probability. If that limit is around 10% and the typical antineutrino energy is taken to be 3 MeV, the experiment is sensitive to differences of squares of masses of roughly 0.7 $\text{eV}^2/L(\text{m})$. For Δm^2 large enough to give many oscillations of the neutrino before detection, the limit on $\sin^2 2\theta$ is twice the limit obtained for the oscillation probability since then the factor $\sin^2[\Delta M^2 L/(4E)]$ averages to one-half. See Figure 16.4.

An experiment performed at the Bugey reactor near Lyon, France observed electron antineutrinos through inverse beta decay: $\overline{\nu}_e p \rightarrow e^+ n$. The positron was observed through scintillation light caused by its two-gamma annihilation with an electron. The neutron was observed by doping the scintillator with Li^6, which is sensitive through the process $n + \text{Li}^6 \rightarrow \text{He}^4 + \text{H}^3 + \gamma(4.8\ \text{MeV})$. The primary observations were made at distances of 15 m and 40 m from a 2.8 GW reactor. Oscillation of the electron antineutrinos would have led to a reduced event rate. As reported in 1994/5, no reduction was observed at the few percent level, excluding values of Δm^2 on the scale of 0.02 eV^2.

To improve upon this it was necessary to make measurements further from a reactor. A nuclear power station located near Chooz in the Ardennes region of France served as

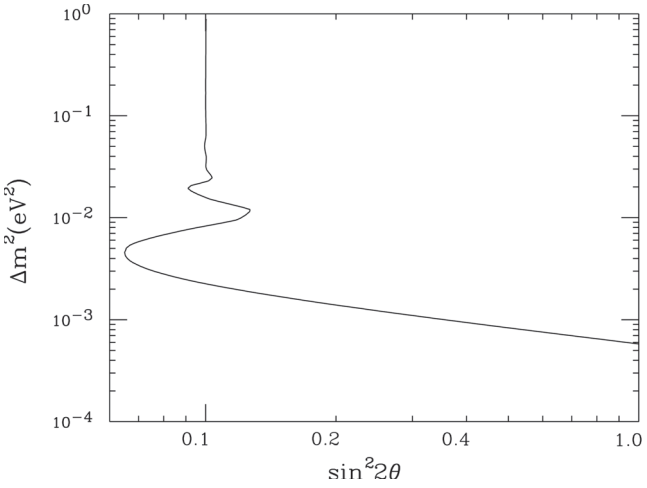

Figure 16.4. Reactor neutrino experiments give limits on Δm^2 and $\sin^2 2\theta$. A limit on the fraction of the $\overline{\nu}_e$ that are transmuted into unobservable $\overline{\nu}_\mu$ restricts the allowed region in the $\Delta m^2 - \sin^2 2\theta$ plane through the relation in Eq. (16.9). The allowed region is to the left and below the curve. The sensitivity to Δm^2 is greatest if $\sin^2 2\theta$ is near unity. If the oscillation probability is shown to be less than P, then the sensitivity extends in eV^2 to about $P^{1/2} < E(\text{MeV}) > /1.27L(\text{m})$, where $< E >$ is the mean neutrino energy. The figure represents an experiment with $L = 1$ km, $< E >= 3.5$ MeV, and $P = 0.05$. In the limit of large Δm^2, the limit on $\sin^2 2\theta$ is $2P$, as shown in the figure.

the antineutrino source for a more precise experiment again relying on inverse beta decay (Ref. 16.3). The neutron was observed by incorporating gadolinium in a liquid scintillator detector, located 1 km from the reactor. Gadolinium has a large cross section for neutron absorption, which is signaled by the emission of a gamma ray of 8 MeV. The neutrons could also be observed by their absorption by protons, producing a deuteron and a 2.2 MeV gamma. The delay of 2 to 100 μs between the positron annihilation and the neutron absorption provided a signature for the events. The signal event rate was found to be proportional to the instantaneous power of the reactor, as it should have been. The value of about 25 neutrino events per day at full power was much larger than the background of about 1 event per day.

The anticipated rate in the absence of neutrino oscillations depended on the intensity and energy spectrum of the neutrinos emitted by the reactor. Including this uncertainty and others associated with the detector, the ratio of the measured to the expected rate reported in 1998 was $0.98 \pm 0.04 \pm 0.04$, where the first error was statistical and the second systematic. Mixing would reduce the ratio by $1 - \frac{1}{2}\sin^2 2\theta$. At 90% CL, the ratio is greater than 0.91, so at the same confidence level, for large Δm^2, $\sin^2 2\theta < 0.18$. Using a mean neutrino energy of 3 MeV and the distance between the reactor and the detector, for $\sin^2 2\theta = 1$ we find the limit $\Delta m^2 < 0.9 \times 10^{-3}$ eV^2. With additional data Chooz reported refined results in 1999: for large Δm^2, $\sin^2 2\theta < 0.10$ and for $\sin^2 2\theta = 1$, $\Delta m^2 < 0.7 \times 10^{-3}$ eV^2, at 90% CL (Ref. 16.4).

Subsequently a similar experiment was conducted at the Palo Verde Generating Station in Arizona with consistent results: for large Δm^2, $\sin^2 2\theta < 0.164$ and for $\sin^2 2\theta = 1$, $\Delta m^2 < 1.1 \times 10^{-3}$ eV^2, at 90% CL.

16.8 SNO

The convincing evidence of atmospheric neutrino oscillations involving ν_μ at Super-Kamiokande intensified interest in the solar ν_e problem. The MSW effect, together with vacuum oscillations provided several possible solutions. An experiment at the Sudbury Neutrino Observatory in Ontario, Canada finally resolved the issue (**Ref. 16.5**).

Like Super-Kamiokande, SNO used a large water-filled detector, but with a difference. The water was not H_2O but D_2O. As in the famous plant at Rjukan, Norway whose heavy water was seized by the Nazis for work on the atomic bomb, Sudbury's heavy water was the result of electrolysis using plentiful and inexpensive hydroelectric power. The advantage of heavy water for solar neutrino experiments is participation of three distinct reactions:

$$\begin{aligned} \nu_e + d &\rightarrow p + p + e^- \quad (CC) \\ \nu_x + d &\rightarrow p + n + \nu_x \quad (NC) \\ \nu_x + e^- &\rightarrow \nu_x + e^- \quad (ES) \end{aligned} \tag{16.20}$$

Only electron-type neutrinos can give the first reaction, while electron-, muon-, and tau-neutrinos can all participate in the last two. In the initial results from SNO, only the charged-current and elastic scattering events were used. If we suppose there are no neutrino oscillations, then the ν_e flux can be inferred from either the charged-current or electron-scattering events since the underlying cross sections are known. Neutrino oscillations would generate a flux of ν_μ and/or ν_τ, which would contribute, through neutral current interactions, to the elastic scattering to give an apparent contribution, at about one-sixth strength, to the ν_e flux inferred in this process. The ν_μ and/or ν_τ would not contribute to the charged-current events.

Slightly fewer than 10,000 phototubes were arrayed to view the heavy water contained within an acrylic vessel, itself surrounded by a shield of ordinary water. Just as for Super-Kamiokande, the detector was sensitive only above a few MeV and thus responded to solar neutrinos from ^{8}B. The energy was determined by counting phototube hits, with about nine hits for each MeV of electron energy. Timing the arrival of the Cherenkov photons allowed determination of the origin of the electron and its direction.

Signals from the charged-current and elastic scattering events were separated from each other and from the neutron background by fitting their distribution in energy released, scattering angle relative to the Sun, and radial distance from the center of the detector. The neutron background occurred predominantly near the periphery of the detector.

Using the anticipated shape of the ^8B spectrum, the full flux of ^8B electron neutrinos could be deduced from the charged-current and elastic scattering processes, with the

results, in units of 10^6 cm^{-2} s^{-1}

$$\phi^{CC} = 1.75 \pm 0.07(\text{stat}) \begin{matrix}+0.12\\-0.11\end{matrix} (\text{syst}) \pm 0.05(\text{theor})$$
$$\phi^{ES} = 2.39 \pm 0.34(\text{stat}) \begin{matrix}+0.16\\-0.14\end{matrix} (\text{syst}) \tag{16.21}$$

suggesting an excess in elastic scattering, which would signal the presence of neutral current scattering from ν_μ and ν_τ. Conclusive evidence came from using the earlier, more precise measurement of elastic scattering by the Super-Kamiokande team, which in the same units was

$$\phi^{ES} = 2.32 \pm 0.03(\text{stat}) \begin{matrix}+0.09\\-0.07\end{matrix} (\text{syst}). \tag{16.22}$$

This, then, established that there were active neutrinos causing elastic scattering and not contributing to the charged-current process. Analyzed in this light, the sum of the fluxes from ν_μ and ν_τ could be determined. It is about twice that in the ν_e flux. If we suppose that MSW is completely effective so $\cos 2\theta_N = -1$, we conclude that $(1 + \cos 2\theta_0)/2 \approx 2/3$ so $\sin^2 2\theta_0 \approx 8/9$, i.e. nearly maximal mixing. For MSW to be complete we need $\Delta M^2 \cos 2\theta_0 < A$. Here θ_0 and ΔM^2 stand for θ_{sol} amd Δm^2_{sol}. The lowest energy neutrinos SNO detected had energies of about 6.75 MeV, so $A \approx 8.5 \times 10^{-5}$ eV^2. This means that $\Delta m^2_{\text{sol}} < 25 \times 10^{-5}$ eV^2. If Δm^2_{sol} were as low as 1×10^{-5} eV^2 then even the pp neutrinos observed by gallium experiments would be similarly MSW suppressed, in disagreement with the data. See Exercise 16.4.

It was the inferred neutral current contribution to elastic scattering that demonstrated flavor oscillations in the 2001 SNO result. Direct observation of the neutral current through $\nu + d \rightarrow p + n + \nu$ at SNO (**Ref. 16.6**) followed in 2002. The challenge here was to detect the neutron through its capture on the deuteron, $n + d \rightarrow t + \gamma$. The 6.25-MeV gamma produced Cherenkov light through its shower. These were excluded in the earlier analysis by setting the threshold at 6.75 MeV. The neutral current disintegration of the deuteron was separated from the charged-current and elastic scattering events by its energy spectrum and angular distribution.

The neutral current measurement is difficult because every free neutron in the heavy-water detector, whether due to the signal or the background, behaves in the same way. The heavy water itself is inevitably contaminated with thorium and uranium, which decay into chains of radioactive daughters. By carefully monitoring these chains, this background could be subtracted. The flux of ν_e and the sum of the ν_μ and ν_τ fluxes could then be determined:

$$\phi_e = 1.76 \begin{matrix}+0.05\\-0.03\end{matrix} (\text{stat}) \begin{matrix}+0.09\\-0.09\end{matrix} (\text{syst})$$
$$\phi_{\mu\tau} = 3.41 \begin{matrix}+0.45\\-0.45\end{matrix} (\text{stat}) \begin{matrix}+0.48\\-0.45\end{matrix} (\text{syst}) \tag{16.23}$$

again in units of 10^6 cm^{-2} s^{-1}, in excellent agreeement with the results of 2001, which relied on the elastic scattering measurement of Super-Kamiokande.

16.9 KamLAND

The SNO results showed that solar neutrinos indeed mix. To reach much lower values of Δm^2 than explored at Chooz, it was necessary to place a detector much further from the reactor. The Kamioka Liquid Scintillator Anti-Neutrino Detector (KamLAND) was built at the site previously used by the Kamiokande experiment, under rock equivalent to 2700 meters of water. This location is surrounded by 53 Japanese nuclear power reactors, with 79% of the neutrino flux coming from 26 of those reactors located at distances from 138 km to 214 km. As at Chooz, the signal for $\overline{\nu}_e p \rightarrow e^+ n$ was the positron annihilation followed by a gamma from neutron capture. To compensate for the much diminshed antineutrino flux so far from the reactors, the detector was on a grand scale: a kiloton of liquid scintillator, of which about 50% lay inside the fiducial volume, about 100 times the target used at Chooz. Despite this, the event rate at KamLAND was about half an event per day compared to 25 events per day at Chooz. It was for this reason that it was necessary that it be shielded from cosmic ray background by going deep underground.

In its initial report in 2003 (Ref. **16.7**), the KamLAND experiment had 54 events, an estimated single event from background, and a total expected in the absence of oscillations of 86.8 ± 5.6. The ratio of observed to expected rates was given as $0.611 \pm 0.085(\text{stat}) \pm 0.041(\text{syst})$. This required that $\sin^2 2\theta_{\text{sol}}$ be greater than about 0.25 at 95% CL, but allowed any value of Δm^2_{sol} greater than about 10^{-5} eV^2. Because the disappearance probability depends directly on the incident antineutrino energy, the spectrum of energies observed should be distorted from the initial spectrum by the oscillations. By fitting to the energy spectrum KamLAND was able to determine best values for $\sin^2 2\theta_{\text{sol}}$ and Δm^2 separately, with the results $\sin^2 2\theta_{\text{sol}} = 1.0$, $\Delta m^2_{\text{sol}} = 6.9 \times 10^{-5}$ eV^2. This result was decisive in choosing the large mixing angle (LMA) solution for the solar neutrino puzzle.

KamLAND reported again in 2005, with much increased statistics (Ref. 16.8). The number of signal events with backgrounds subtracted was near 240 while the expectation in the absence of oscillations was 356 ± 24. With this much larger sample it was possible to establish the oscillatory behavior of the energy spectrum as a function of $1/E$. From the KamLAND data alone, Δm^2_{sol} was determined to be $7.9^{+0.6}_{-0.5} \times 10^{-5}$ eV^2 with $\tan^2 \theta_{\text{sol}} \approx 0.46$. Including solar neutrino data determined $\tan^2 \theta_{\text{sol}} = 0.40^{+0.10}_{-0.07}$, i.e. $\sin^2 2\theta_{\text{sol}} = 0.82 \pm 0.07$. A much larger sample with more that 1600 events collected through May 2007 showed nearly two cycles of oscillation, once the effect of antineutrinos from terrestrial sources were taken into account. See Figure 16.5. The KamLAND results significantly tightened the limits on Δm^2_{sol}. Combining with results from solar neutrino experiments gave $\Delta m^2_{\text{sol}} = (7.59 \pm 0.21) \times 10^{-5}$ eV^2 and $\tan^2 \theta_{\text{sol}} = 0.47^{+0.06}_{-0.05}$.

16.10 Investigating Atmospheric Neutrino Oscillations with Accelerators

Despite the remarkable achievements of Super-Kamiokande, it was inevitable that accelerators would eventually seize center stage. Cosmic rays provide unmatched reliability: they never shut down. But a neutrino beam produced by decaying pions and kaons has a well-defined direction and a relatively small range in energy. The oscillations of atmospheric neutrinos gave $\Delta m^2_{\text{atm}} \approx 3 \times 10^{-3}$eV^2, so from Eq. (16.9), to see the effect we

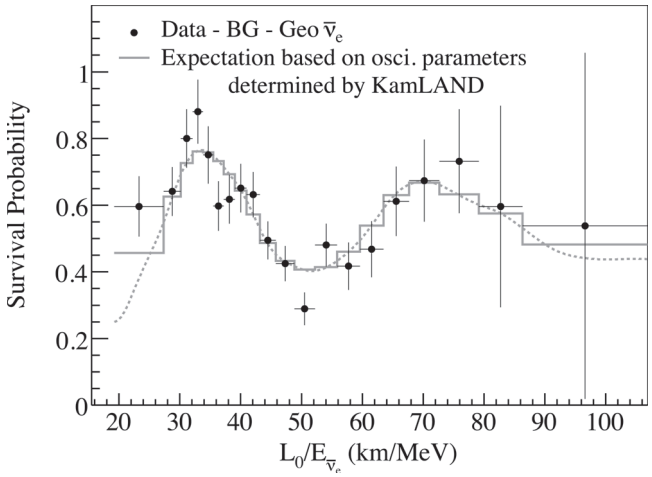

Figure 16.5. The survival probability of $\bar{\nu}_e$ as measured by KamLAND (Ref. 16.9). Backgrounds, including terrestrial antineutrinos, have been subtracted. The baseline $L_0 = 180$ km is the result of weighting contributions from the various contributing reactors in Japan.

need $E/L \approx (1\,\text{GeV}/300\,\text{km})$. Certainly the detector cannot be located at the accelerator itself!

Aiming a beam from the 12-GeV proton synchroton at KEK in Tsukuba at the Super-Kamiokande detector 250 km away provides an excellent match to these requirements. A detector located just 300 meters from the target provided a means of monitoring the neutrino beam. Data from two years' running, beginning in June 1999 and reported in 2003 (Ref. 16.10) produced 56 muon events against an expectation of $80^{+6.2}_{-5.4}$ in the absence of oscillation. The energy distribution of the events was also distorted from the spectrum expected without oscillations. While the best fit to the data gave $\sin^2 2\theta_{\text{atm}}$ very near unity and $\Delta m^2_{\text{atm}} = 2.7 \times 10^{-3}\,\text{eV}^2$, the values were poorly determined. With approximately twice the data, in 2006 K2K reported essentially the same central value, but with a much narrower range, $1.9 \times 10^{-3}\ \text{eV}^2 < \Delta m^2_{\text{atm}} < 3.5 \times 10^{-3}\ \text{eV}^2$ (Ref. 16.11), and again $\sin^2 2\theta_{\text{atm}}$ very near unity.

The MINOS (Main Injector Neutrino Oscillation Search) at Fermilab used a much more energetic beam, 120-GeV protons, to create a neutrino beam maximized at energies between 1 and 3 GeV (Ref. 16.12). The far detector was located in the Soudan iron mine, 735 kilometers away in Minnesota and had a more conventional structure for an accelerator experiment. The muons were observed with steel plates and scintillator, read out with photomultiplier tubes. A near detector, one kilometer from the origin of the neutrino beam, had the same construction.

The much higher energy proton beam produced neutrinos up to 30 GeV and beyond, but it was the lower energy neutrinos that provided the most useful information. Neutral-current events were separated from the charged-current events by the pattern of energy deposition in the detector. The disappearance of muons was apparent: below 10 GeV 122 muon events were seen when 238 ± 11 would have been expected in the absence of

oscillations. The results for the mixing parameters were quite similar to those obtained by K2K and Super-Kamiokande: 2.31×10^{-3} eV^2 $< \Delta m^2_{\rm atm} < 3.43 \times 10^{-3}$ eV^2 and $\sin^2 2\theta_{\rm atm} > 0.78$ at 90% CL. When data taken through July 2007 were included, these limits were significantly improved to $\Delta m^2_{\rm atm} = (2.43 \pm 0.13) \times 10^{-3}$ eV^2 and $\sin^2 2\theta_{\rm atm} > 0.90$ at 90% CL (Ref. 16.13).

16.11 Neutrinos from Low-Energy Muons

Accelerators produce primarily ν_μ, which result from the decays $\pi^+ \to \mu^+\nu_\mu$ and $K^+ \to \mu^+\nu_\mu$, and $\overline{\nu}_\mu$ from the analogous decays of negative particles. The semileptonic decay $K^+ \to \pi^0 e^+ \nu_e$ has a 4% branching ratio and is an unfortunate contaminant.

By working with a low-energy primary proton beam, K production can be excluded. The dominance of the decay $\pi^+ \to \mu^+\nu_\mu$ guarantees a nearly pure ν_μ beam with little $\overline{\nu}_\mu$ contamination since the muon is so long-lived. On the other hand, a pure μ^+ beam that is stopped in matter will produce a pure $\overline{\nu}_\mu$ source without a ν_μ component. This provides the means to search for both $\overline{\nu}_\mu \to \overline{\nu}_e$ and $\nu_\mu \to \nu_e$ oscillations. The Liquid Scintillator Neutrino Detector (LSND) (Ref. 16.14) at Los Alamos looked for evidence for both kinds of oscillations.

LSND took data from 1993 and through 1998. Oscillations of $\overline{\nu}_\mu \to \overline{\nu}_e$ could be detected by observing $\overline{\nu}_e p \to e^+ n$, with the e^+ producing Cherenkov light and the neutron yielding a 2.2 MeV photon through $np \to d\gamma$. The essence of the experiment is to eliminate background $\overline{\nu}_e$ or other particles that might produce similar events in the liquid scintillator, which is viewed with photomultiplier tubes. The initiating proton beam energy was only 800 MeV, leading to many fewer negative pions being produced than positive pions. Most negative pions were absorbed by nuclei before they could decay weakly; the remaining ones would give a negative muon and subsequently $e^- \nu_\mu \overline{\nu}_e$, if the muon was not absorbed first. A larger source of background was not associated with the beam and could be estimated by measuring the event rate between accelerator pulses.

In 1995, the experiment reported that with stringent requirements on the gamma identification, there were 9 events, with an expected background of 2.1, giving a probability that this was a statistical fluctuation of less than 10^{-3}. Fitting to a larger sample obtained by relaxing some criteria gave an oscillation probability of $(0.34^{+0.20}_{-0.18} \pm 0.07) \times 10^{-2}$. If the neutrinos make many oscillations in the 30 meters between the neutrino source and the detector, then this would indicate $\sin^2 2\theta \approx 6.8 \times 10^{-3}$. The minimal Δm^2 consistent with the data is found by setting the mixing to its maximum, $\sin^2 2\theta = 1$, and if we take $E \approx 45$ MeV and $L \approx 30$ m, we find $\Delta m^2 > 0.07$ eV^2. A final report in 2001(Ref. 16.15) gave a consistent result, with 118 ± 22 events against an expected background of 30 ± 6 and an oscillation probability of $(0.264 \pm 0.067)\%$.

The decay in flight of pions produced at LAMPF generated a beam of ν_μ whose energy spectrum extended beyond 200 MeV. The transformation $\nu_\mu \to \nu_e$ would be signaled by electrons produced in carbon targets through $\nu_e C \to e^- X$. By looking for electrons with energy between 60 and 200 MeV it was possible to exclude events generated by muon decay at rest. An analysis of the data from 1993 to 1995 found an excess of 18.1 ± 6.6

events and an oscillation probability of $(2.6 \pm 1.0 \pm 0.5) \times 10^{-3}$, very close to the result obtained from decays at rest. The final analysis (Ref. 16.15), however, was ambiguous. The excess was 14.7 ± 12.2 events, with a background of 6.6 ± 1.7 events, altogether a transition probability of (0.10 ± 0.16) %, consistent both with no oscillations and with the positive result found in decay-at-rest. The result combining both decays at rest and decays in flight indicated that at 90% CL, both $\Delta m^2 > 0.02\ \mathrm{eV}^2$ and $\sin^2 2\theta > 10^{-3}$.

The LSND result was incompatible with the three-neutrino pictures because with just three neutrinos there can be only two independent mass-squared differences. To account for the solar neutrino mass-squared splitting near $8 \times 10^{-5}\,\mathrm{eV}^2$, the atmospheric mass-squared splitting near $3 \times 10^{-3}\,\mathrm{eV}^2$ and the LSND splitting near $0.1\,\mathrm{eV}^2$ would require introducing a fourth neutrino. This neutrino would have to be sterile: it couldn't couple to the Z, whose width showed that it coupled to precisely three neutrinos.

The MiniBooNE experiment (Ref. 16.16) at Fermilab was designed to confirm or contradict the LSND result. An 8-GeV proton beam impinging on beryllium generated pions and kaons. A toroidal magnetic field focused the positive particles. Their decays produced a neutrino beam dominated by ν_μ, which interacted in a detector 541 meters away. The Cherenkov and scintillation light from the charged particles produced in these interactions were viewed by 1280 8-inch photomultiplier tubes.

The neutrino beam energy was centered at 700 MeV. At this low energy the dominant reactions were $\nu_\mu n \to \mu^- p$, $\nu_\mu N \to \nu_\mu N$, $\nu_\mu N \to \mu^- N\pi$ and $\nu_\mu N \to \nu_\mu N\pi$. If the LSND result were correct, about 0.26% of the ν_μ would be transmuted into ν_e and the analogous charged current interactions would produce electrons in place of muons. Electrons and muons produced different patterns of light, which could be distinguished by the collection of PMTs. Some background events were expected from ν_e contamination of the neutrino beam as a result of K^+ and K_L decays and from muon decays. Produced π^0 also contributed because their decay photons gave a signal similar to that of an electron. In charged current interactions, the energy of the charged lepton was determined from the signals recorded by the PMTs. The energy of the incident neutrino was deduced from the angle the lepton made with the incident neutrino direction and from the observed lepton energy. Simple events $\nu_\mu n \to \mu^- p$ in which the muon decayed in the detector volume and the resulting electron was observed provided a powerful check on the procedures.

A fit was made to the data for events with an observed electron as a function of the incident neutrino energy. Without revealing to themselves the parameters determined by the neutrino-oscillation fit, the MiniBooNE team examined the quality of the fit. Discrepancies in the numbers of events in the low-energy bins led to a decision to restrict the fit to neutrino energies about 475 MeV. Once this was done, the fit with no oscillations was found to give a χ^2 probability 93% indicating no need to include oscillations, in contradiction with the LSND results.

16.12 Oscillations Among Three Neutrino Types

Neutrino oscillation phenomena have been described above as if each involved only two species, though that is clearly incorrect. Evidence from the atmospheric neutrinos showed

a mass-squared difference of about 2.5×10^{-3} eV^2, while that in solar neutrinos is about 8×10^{-5} eV^2. Thus there must be two mass-eigenstate neutrinos separated in mass-squared by the smaller amount, and a third mass eigenstate separated from the first two by the larger amount.

Now there appears to be a puzzle in that the Chooz reactor experiment indicated that $\Delta M^2_{\text{Chooz}} < 10^{-3}$ eV^2 while the atmospheric experiment found a larger value in the oscillations of ν_μ. This is resolved if we suppose that ν_e is mostly made of the two neutrinos with similar masses, ν_1 and ν_2. Then experiments, like Chooz and solar neutrino measurements, will depend nearly entirely on this two-state system, characterized by a small value for $\Delta M^2 = \Delta m^2_{\text{sol}}$. This justifies the treatment of solar neutrinos as a two-state system.

The MNS matrix U, which changes flavor eigenstates $|\nu_\alpha\rangle$ into mass eigenstates $|\nu_i\rangle$, $\sum_\alpha |\nu_\alpha\rangle U_{\alpha,i} = |\nu_i\rangle$ can be written as

$$\begin{bmatrix} \nu_1 & \nu_2 & \nu_3 \end{bmatrix} = \begin{bmatrix} \nu_e & \nu_\mu & \nu_\tau \end{bmatrix} U \tag{16.24}$$

where

$$U = \begin{bmatrix} c_{12}c_{13} & s_{12}c_{13} & s_{13}e^{-i\delta} \\ -s_{12}c_{23} - c_{12}s_{23}s_{13}e^{i\delta} & c_{12}c_{23} - s_{12}s_{23}s_{13}e^{i\delta} & s_{23}c_{13} \\ s_{12}s_{23} - c_{12}c_{23}s_{13}e^{i\delta} & -c_{12}s_{23} - s_{12}c_{23}s_{13}e^{i\delta} & c_{23}c_{13} \end{bmatrix}$$

$$\times \begin{bmatrix} e^{i\alpha_1/2} & 0 & 0 \\ 0 & e^{i\alpha_2/2} & 0 \\ 0 & 0 & 1 \end{bmatrix}. \tag{16.25}$$

Here we have introduced the angles θ_{ij}, $i < j$ and $s_{ij} = \sin\theta_{ij}, c_{ij} = \cos\theta_{ij}$. This has the same form as the CKM matrix, except for the additional angles α_1 and α_2. These change the phase of the Majorana neutrinos 1 and 2. Ordinarily such a phase would be irrelevant because usually a state and its conjugate with the opposite phase will occur. However, Majorana neutrinos are their own conjugates. In neutrinoless double beta decay, these phases have observable consequences, though they do not affect neutrino oscillations.

The meaning of the angles θ_{ij} is clearer if we write, dropping the αs

$$U = \begin{bmatrix} 1 & 0 & 0 \\ 0 & c_{23} & s_{23} \\ 0 & -s_{23} & c_{23} \end{bmatrix} \begin{bmatrix} c_{13} & 0 & s_{13}e^{-i\delta} \\ 0 & 1 & 0 \\ -s_{13}e^{i\delta} & 0 & c_{13} \end{bmatrix} \begin{bmatrix} c_{12} & s_{12} & 0 \\ -s_{12} & c_{12} & 0 \\ 0 & 0 & 1 \end{bmatrix}. \tag{16.26}$$

The amount of ν_3 in the electron neutrino is governed by θ_{13}. The Chooz experiment shows that it is small. However, it is this small entity in the MNS matrix that carries the CP violation that can be seen in oscillation experiments like $\nu_\mu \to \nu_e$ vs $\overline{\nu}_\mu \to \overline{\nu}_e$.

In the limit of small θ_{13}, solar neutrino oscillations are described by θ_{12}. The oscillations occur between ν_e and the combination $\nu_x = c_{23}\nu_\mu - s_{23}\nu_\tau$. The angle θ_{23} cannot be studied in solar neutrino reactions because low energy ν_μ and ν_τ behave identically.

In atmospheric neutrino experiments, where $\Delta M^2 = \Delta m^2_{\rm atm} \approx 2.5 \times 10^{-3}\,{\rm eV}^2$ governs, the small mass-squared splitting between ν_1 and ν_2 cannot be seen, so θ_{12} does not influence the behavior. If we set it to zero, and again drop θ_{13} as being small, we see that θ_{23} is the mixing angle for the cosmic-ray experiments like Super-Kamiokande.

Both θ_{12} and θ_{23} are large, while θ_{13} is small. However, it is this small entity in the MNS matrix that carries the CP violation that could be seen in oscillation experiments like $\nu_\mu \to \nu_e$ vs $\overline{\nu}_\mu \to \overline{\nu}_e$. See Exercise 16.7 and 16.8. The differences of squares of neutrino masses are simply related to the values of ΔM^2 found in the solar and atmospheric neutrino oscillations: $\Delta m^2_{\rm sol} = m_2^2 - m_1^2$, $\Delta m^2_{\rm atm} = |m_3^2 - m_1^2| \approx |m_3^2 - m_2^2|$.

Three fundamental questions remain in neutrino physics: the values of $\sin 2\theta_{13}$ and δ, and whether the two nearly equal-mass states lie above or below the third mass eigenstate. One possibility for the CP violation required to explain the baryon–antibaryon asymmetry of the universe is that it derives ultimately from CP violation in the decays of the extremely heavy neutrinos that are the see-saw partners of the ordinary neutrinos. Measuring CP violation in the interactions of the light neutrinos would provide some circumstantial evidence for CP violation in the inaccessible neutrinos.

Exercises

16.1 Estimate the flux of solar neutrinos from the $pp \to de^+\nu_e$ process at the surface of the Earth using the surface temperature of the Sun, 5777 K, and its surface area, 6.1×10^{18} m^2. The overall primary cycle initiated by the pp process is

$$4p \to {\rm He}^4 + 2e^+ + 2\nu_e$$

whereby about 26.1 MeV is generated, aside from that carried away by the neutrinos themselves. Remember that the energy emission per unit area from a black body is $J = \sigma T^4$, where the Stefan–Boltzmann constant is

$$\sigma = \frac{\pi^2 k^4}{60\hbar^3 c^2} = 5.67 \times 10^{-8}\ {\rm Wm}^{-2}({\rm deg\ K})^{-4}.$$

16.2 Verify the numerical relation in Eq. (16.12). Verify the claim that an electron-neutrino would accumulate a phase of 2π from the MSW effect traversing 1.6×10^4 km of hydrogen with a density of 1 g cm^{-3}.

16.3 For the SNO detector described in **Ref. 16.3**, estimate the energy resolution using Poisson statistics and the mean number of PMT hits per MeV of electron energy. Compare with the detailed fit to the resolution given in the paper.

16.4 Calculate the suppression of solar neutrinos by mixing and the MSW effect as a function of the neutrino energy taking $\tan\theta_0 = 0.47$ as suggested by the KamLAND data. Assume the problem can be treated as involving only two neutrino species. Take $\Delta M_0^2 = 8 \times 10^{-5}$ eV^2. Use Table 16.1. Assume that the "other" contributions (from ^{13}N, ^{15}O and pep) are concentrated near 1 MeV. Determine the quality of the fit to the gallium and chlorine data.

16.5 Show that in the three neutrino scheme, the probability of oscillation from α to β is

$$P(\nu_\alpha \to \nu_\beta) = \delta_{\alpha\beta} - 4\sum_{i>j} \Re(U^*_{\alpha i} U_{\beta i} U_{\alpha j} U^*_{\beta j}) \sin^2\left(\frac{\Delta m^2_{ij} L}{4E}\right) + 2\sum_{i>j} \Im(U^*_{\alpha i} U_{\beta i} U_{\alpha j} U^*_{\beta j}) \sin\left(\frac{\Delta m^2_{ij} L}{2E}\right).$$

CPT requires $P(\overline{\nu}_\alpha \to \overline{\nu}_\beta) = P(\nu_\beta \to \nu_\alpha)$. The expression for $P(\overline{\nu}_\alpha \to \overline{\nu}_\beta)$ is obtained from $P(\nu_\alpha \to \nu_\beta)$ by replacing U with U^*.

16.6 Use the result above to show that in a neutrino reactor experiment aimed at measuring $\sin^2\theta_{13}$ where $\Delta m^2_{31} L/(4E) \approx \pi/2$, the survival probability is given by

$$P(\overline{\nu}_e \to \overline{\nu}_e) = 1 - \sin^2 2\theta_{12} \sin^2 \frac{\Delta m^2_{21} L}{4E} - \sin^2 2\theta_{13} \sin^2 \frac{\Delta m^2_{31} L}{4E}.$$

In an experiment with $\Delta m^2_{31} L/(4E) \gg 1$ designed, like KamLAND, to measure Δm^2_{21} and $\sin^2 2\theta_{12}$, the appropriate approximation is

$$P(\overline{\nu}_e \to \overline{\nu}_e) = \cos^4\theta_{13} \left[1 - \sin^2 2\theta_{12} \sin^2 \frac{\Delta m^2_{21} L}{4E}\right].$$

16.7 Verify that

$$\begin{aligned} P(\nu_\mu \to \nu_e) = {} & \sin^2\theta_{23}\ \sin^2 2\theta_{13}\ \sin^2\Delta_{31} \\ & + \sin 2\theta_{13}\Delta_{21} \sin 2\theta_{12}\ \sin 2\theta_{23} \sin\Delta_{31} \cos(\Delta_{31} + \delta) \\ & + \Delta^2_{21} \cos^2\theta_{23} \sin^2 2\theta_{12} \end{aligned}$$

where $\Delta_{ij} = \Delta m^2_{ij} L/(4E)$ and where $\sin 2\theta_{13}$, Δ_{21} and $|\Delta m^2_{21}/\Delta m^2_{31}|$ are treated as small. For $\overline{\nu}_\mu \to \overline{\nu}_e$ the sign of δ is reversed. Using the experimental values for Δm^2_{31} and Δm^2_{21}, determine the size of the CP asymmetry

$$A = \frac{P(\nu_\mu \to \nu_e) - P(\overline{\nu}_\mu \to \overline{\nu}_e)}{P(\nu_\mu \to \nu_e) + P(\overline{\nu}_\mu \to \overline{\nu}_e)}.$$

Evaluate as a function of $\sin 2\theta_{13}$ and δ. Assume $\sin^2 2\theta_{12} = 0.82$, $\sin^2 2\theta_{23} = 1.0$, and suppose $\Delta_{31} = \pi/2$ so that the asymmetry is maximized.

16.8 If the neutrinos in Exercise 16.7 are not traveling in vacuum, but in a material with electron density N_e, the oscillation probability is instead given by

$$P(\nu_\mu \to \nu_e) = \sin^2\theta_{23}\,\sin^2 2\theta_{13}\,\frac{\sin^2(1-x)\Delta_{31}}{(1-x)^2} + \frac{\Delta m^2_{21}}{\Delta m^2_{31}}\sin 2\theta_{13}\sin 2\theta_{12}\,\sin 2\theta_{23}\frac{\sin[(1-x)\Delta_{31}]}{1-x}\frac{\sin x\Delta_{31}}{x}\cos(\Delta_{31}+\delta) + \left(\frac{\Delta m^2_{21}}{\Delta m^2_{31}}\right)^2\cos^2\theta_{23}\sin^2 2\theta_{12}\frac{\sin^2(x\Delta_{31})}{x^2}$$

where $x = 2\sqrt{2}G_F N_e E/\Delta m^2_{31}$ and where non-leading terms in $\Delta m^2_{21}/\Delta m^2_{31}$ and θ_{13} have been neglected. Show that for rock with a density of about 2.4 g/cm^3, $x \approx E(\text{GeV})/14$ if Δm^2_{31} is positive.

Introduce the variables $x = \sin 2\theta_{13}\cos\delta$, $y = \sin 2\theta_{13}\sin\delta$. Take Δm^2_{21}, $|\Delta m^2_{31}|$, $\sin 2\theta_{12}$ and $\sin 2\theta_{13}$ as known. Show that for given E and L, the equations $P(\nu_\mu \to \nu_e) = C_1$ and $P(\overline{\nu}_\mu \to \overline{\nu}_e) = C_2$ give circles in the x–y plane. What are the radii and centers of the circles? For the antineutrino case, $\Delta_{31}+\delta$ becomes $\Delta_{31}-\delta$. The sign of x is reversed for the antineutrino case because the antineutrino has a potential opposite that for a neutrino in matter. How are the equations changed if the neutrino spectrum is inverted and how is this reflected in the pattern of the circles in the x–y plane?

16.9 Neutrino beams are formed by focusing pions produced in high energy proton collisions with a fixed target. Pions of a single charge are focused toward the forward direction with a magnetic field. In an idealized description all the pions are moving along a single axis. A single pion of energy $E_\pi = \gamma m_\pi$ decays isotropically in its own rest frame to $\mu\nu_\mu$. Show that in the high energy limit, the distribution of neutrinos in the lab frame is

$$\frac{dN}{d\phi\, d\cos\theta_{lab}} = \frac{4\gamma^2}{(1+\gamma^2\theta^2_{lab})^2}\frac{1}{4\pi}$$

where we assume $\theta_{lab} << 1$. The maximum transverse momentum of the neutrino is $p^* = (m^2_\pi - m^2_\mu)/(2m_\pi)$. At a fixed θ_{lab}, what is the highest neutrino energy, E_ν^{max}? For fixed θ_{lab} and neutrino energy $E_\nu < E_\nu^{max}$, pions of two distinct energies may contribute, corresponding to decays in the forward and backward hemispheres in the pion rest frame. Show that the requried values of γ are

$$\gamma^{\pm}\theta_{lab} = \frac{E_\nu^{max}}{E_\nu} \pm \sqrt{\left(\frac{E_\nu^{max}}{E_\nu}\right)^2 - 1}.$$

Suppose that the produced pions have a distribution $dN/d\gamma$ where $\gamma = E_\pi/m_\pi$. Show that the spectrum of neutrinos through a detector of area A at a distance R from the source and at an angle θ_{lab} is

$$\frac{dN}{dE_\nu} = \frac{1}{\theta_{lab}^3 E_\nu^{max}} \frac{A}{4\pi R^2} \left\{ \frac{E_\nu^{max}/E_\nu}{\sqrt{\left(\frac{E_\nu^{max}}{E_\nu}\right)^2 - 1}} \left[\frac{dN}{d\gamma}(\gamma^+) + \frac{dN}{d\gamma}(\gamma^-) \right] + \left[\frac{dN}{d\gamma}(\gamma^+) - \frac{dN}{d\gamma}(\gamma^-) \right] \right\}.$$

Show that in the very forward direction, this reduces to

$$\frac{dN}{dE_\nu}(\theta = 0) = \frac{A}{4\pi R^2} \frac{E_\nu^2}{2p^{*3}} \frac{dN}{d\gamma}(\gamma = \frac{E_\nu}{2p^*}).$$

Suppose the neutrino spectrum in the forward direction has the parabolic form $dN/dE \propto E(E_0 - E)$ with $E_0 = 6$ GeV. What will the neutrino spectrum look like at angles $\theta_l = 7,\ 14,\ 27$ mr off-axis?

16.10 Neutrinoless double beta decay depends on the Majorana masses of the neutrinos and the MNS mixing matrix. The decay amplitude is proportional to the effective neutrinoless double beta decay Majorana mass

$$m_{\beta\beta} \equiv \sum_i m_i U_{ei}^2.$$

In standard spectrum the two states with similar mass lie below the third state. In the inverted spectrum the two states with similar mass lie above the third. Since only differences of masses squared have been measured, the mass m^* of the lightest state is unknown. Determine the maximum and minimum values of $|m_{\beta\beta}|$ as a function of m^* for the standard and inverted spectra. Take as representative values $\tan^2\theta_{12} = 0.40$, $\sin^2 2\theta_{13} = 0.10$, $\Delta m_{31}^2 = 2.5 \times 10^{-3}\,\text{eV}^2$, $\Delta m_{31}^2 = 8.5 \times 10^{-5}\,\text{eV}^2$. The values of the phases α_1, α_2, and δ of the MNS matrix are not known and may be varied freely to obtain the maximal and minimal values of $m_{\beta\beta}$. Show that there are values of m^* for the standard spectrum where there is no lower bound to $m_{\beta\beta}$. What upper limit on $m_{\beta\beta}$ would exclude the possibility that neutrinos are Majorana with an inverted spectrum? Graph the allowed regions of $m_{\beta\beta}$ as a function of m^* using a linear plot to simplify the work.

Further Reading

Convenient reviews of many aspects of neutrino oscillations are given in the current *Review of Particle Physics*.

References

16.1 R. Davis, Jr., D. S. Harmer, and K. C. Hoffman, "Search for Neutrinos from the Sun." *Phys. Rev. Lett.*, **20**, 1205 (1968).

16.2 Super-Kamiokande Collaboration, "Evidence for Oscillation of Atmospheric Neutrinos." *Phys. Rev. Lett.*, **81**, 1562 (1998).

16.3 M. Apollonio *et al.*, "Initial Results from the CHOOZ Long Baseline Reactor Neutrino Experiment." *Phys. Lett.*, **420**, 397 (1998).

16.4 M. Apollonio *et al.*, "Limits on Neutrino Oscillations from the CHOOZ Experiment." *Phys. Lett.*, **466**, 415 (1999).

16.5 SNO Collaboration, "Measurement of the Rate of $\nu_e + d \rightarrow p + p + e^-$ Interactions Produced by ^{8}B Solar Neutrinos at the Sudbury Neutrino Observatory." *Phys. Rev. Lett.*, **87**, 071301 (2001).

16.6 SNO Collaboration, "Direct Evidence for Neutrino Flavor Transformation from Neutral-Current Interactions in the Sudbury Neutrino Observatory." *Phys. Rev. Lett.*, **89**, 011301 (2002).

16.7 KamLAND Collaboration, "First Results from KamLAND: Evidence for Reactor Anti-Neutrino Disappearance." *Phys. Rev. Lett.*, **90**, 021802 (2003).

16.8 KamLAND Collaboration, "Measurement of Neutrino Oscillation with KamLAND: Evidence of Spectral Distortion." *Phys. Rev. Lett.*, **94**, 081801 (2005).

16.9 KamLAND Collaboration, "Precision Measurement of Neutrino Oscillation Parameters with KamLAND." *Phys. Rev. Lett.*, **100**, 221803 (2008).

16.10 K2K Collaboration, "Indications of Neutrino Oscillation in a 250 km Long-Baseline Experiment." *Phys. Rev. Lett.*, **90**, 041801 (2003).

16.11 K2K Collaboration, "Measurement of neutrino oscillation by the K2K experiment." *Phys. Rev.*, **D74**, 072003 (2006).

16.12 D. G. Michael *et al*. MINOS, "Observation of Muon Neutrino Disappearance with the MINOS Detectors in the NuMI Neutrino Beam." *Phys. Rev. Lett.*, **97**, 191801 (2006).

16.13 P. Adamson *et al*. MINOS, "Measurement of Neutrino Oscillations with the MINOS Detectors in the NuMI Beam." *Phys. Rev. Lett.*, **101**, 131802 (2008).

16.14 C. Athanassopoulous *et al*. (LSND), "Candidate Events in a Search for $\overline{\nu}_\mu \rightarrow \overline{\nu}_e$ Oscillations." *Phys. Rev. Lett.*, **75**, 2650 (1995).

16.15 A. Aguilar *et al*. (LSND), "Evidence for Neutrino Oscillations from the Observation of $\overline{\nu}_e$ Appearance in a $\overline{\nu}_\mu$ Beam." *Phys. Rev.*, **D64**, 112007 (2001).

16.16 A. A. Aguilar-Arevalo *et al*. (MiniBooNE), "Search for Electron Neutrino Appearance at the $\Delta m^2 \approx 1$ eV^2 Scale." *Phys. Rev. Lett.*, **98**, 231801 (2007).